Longest continuous ground-based measurements of mesospheric CO

Peter Forkman, Patrick Eriksson, and Anders Winnberg
Onsala Space Observatory, Centre for Astrophysics and Space Science, Chalmers University of Technology, Onsala, Sweden

Rolando R. Garcia and Douglas Kinnison
Atmospheric Chemistry Division, National Center for Atmospheric Research, Boulder, Colorado, USA

Received 15 January 2003; revised 15 April 2003; accepted 18 April 2003; published 27 May 2003.

[1] The longest continuous series of ground-based measurements of mesospheric CO is presented. The continuous data cover the period September 2000 to September 2002. Sporadic measurements from 1988 and 1989 are also reported. The results show a large CO accumulation in the winter mesosphere, which is consistent with generally accepted ideas about the seasonally-varying mean meridional circulation. Comparison of the observations with simulations by the Whole Atmosphere Community Climate Model (WACCM) indicate that the model can reproduce the observed seasonal cycle as well as much of its variability, although calculated columns amounts are smaller than the largest values seen in the data. *INDEX TERMS:* 3332 Meteorology and Atmospheric Dynamics: Mesospheric dynamics; 3367 Meteorology and Atmospheric Dynamics: Theoretical modeling; 6969 Radio Science: Remote sensing. **Citation:** Forkman, P., P. Eriksson, A. Winnberg, R. R. Garcia, and D. Kinnison, Longest continuous ground-based measurements of mesospheric CO, *Geophys. Res. Lett.*, *30*(10), 1532, doi:10.1029/2003GL016931, 2003.

1. Introduction

[2] The primary source of carbon monoxide in the mesosphere is the photolysis of carbon dioxide and the major sink is reaction with OH. The variation of mesospheric CO is controlled by middle atmosphere dynamics since its photochemical lifetime is comparable to the time constants associated with transport processes. The dynamics of the mesosphere include planetary and gravity waves, and a seasonally varying meridional circulation, which is driven mainly by momentum flux divergences due to breaking gravity waves [e.g., *Garcia et al.*, 1992]. CO observations and model simulations have been reviewed by *López-Puertas et al.* [2000], who show that CO exhibits a strong seasonal cycle in the mesosphere and lower thermosphere, with much larger values in winter than in summer. Since CO is a good tracer of middle atmospheric dynamics, it has been used to infer the mesospheric circulation. *Bevilacqua et al.* [1985] measured CO emission at 115.27 GHz and observed large enhancements in CO column within a few days which, after trajectory analysis, could be explained by planetary-wave activity. *Aellig et al.* [1995] made observations with a similar instrument and found variations in column density that, after comparisons with simultaneous LIDAR temperature measurements, they attributed to mixing by breaking gravity waves in the mesosphere, followed by the transport of CO-enriched air from higher altitudes. The Improved Stratospheric and Mesospheric Sounder (ISAMS) onboard the Upper Atmosphere Research Satellite (UARS) made the first global stratospheric/lower mesospheric CO measurements during ~6 months in 1991–1992. *Allen et al.* [1999] used ISAMS CO data to examine planetary wave activity in the Arctic upper stratosphere and lower mesosphere.

[3] In this study we present CO total column estimates from continuous ground-based measurements for October 2000 to September 2002, and from sporadic observations made in 1988 and 1989. Due to improvements of the receiver stability during 2001 we also present CO vertical profiles for September 2001 to September 2002. The measurements are compared with results from the Whole Atmosphere Community Climate Model (WACCM), described in Section 4. Figure 1 shows zonal mean profiles of CO number density near 58°N for summer and winter calculated with WACCM. The expected seasonal dependence of CO is clearly seen in these model profiles. The higher number density in the summer lower thermosphere is due to the faster production rate in this season; downwelling of CO-rich air from the thermosphere explains CO accumulation in the wintertime mesosphere and the upper stratosphere.

2. Instrumentation and Observations

[4] For all our observations we measured CO J = 1 → 0 emission at 115.271 GHz with a cooled, 20 K Schottky mixer, operating in frequency-switched single sideband mode with a receiver temperature of ~320 K at Onsala Space Observatory (57.4°N, 12°E). During 1988–89 CO was sporadically measured with the 20-m millimetre-wavelength telescope. Since 2000 we have used the Schottky mixer for almost daily four-hour CO measurements at a constant elevation angle of 90° with a 20-MHz, 800-delay channel autocorrelator spectrometer. We regularly calibrate the instrument with two absorber loads, at 77 K and ambient temperature, respectively. In-between the calibration measurements the receiver noise temperature is assumed to be constant, which is a sufficient assumption to determine the brightness temperatures of the atmosphere. This simplification together with a contribution from an incorrect compensation for the tropospheric attenuation, gives a total estimated calibration error of 5%. The instrument, and the measurement technique are described in *Forkman* [2000].

3. Data Analysis

[5] Figure 2 shows a four-hour spectrum taken on 30 April 2002 together with a fitted spectrum. Column den-

0094-8276/03/2003GL016931$05.00

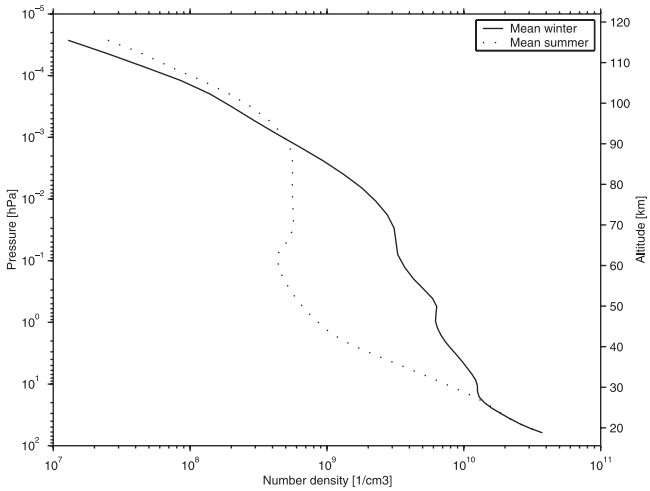

Figure 1. Mean winter and summer CO number densities [cm^{-3}] from WACCM plotted as a function of altitude.

sities above a lower-altitude pressure level can be calculated by integrating the area under the spectrum [*Clancy et al.*, 1984]. The column density, N, is then calculated by

$$N = \frac{\sum_{\nu_c-\nu_o}^{\nu_c+\nu_o} T_b \Delta\nu}{S(\overline{T})\overline{T}} \quad (1)$$

where T_b is the corrected brightness temperature, is the spectral resolution, ν_c is the centre frequency, ν_o gives the frequency range for the integration, S is the transition intensity (from the Jet Propulsion Laboratory spectral line catalogue) and $\overline{T}$ is the mean mesospheric temperature, calculated by weighting the WACCM temperature profile between 60 and 110 km with a CO model profile. If the receiver frequency response is stable and well known it is possible to estimate the natural broadening of the observed line shape and to calculate vertical profiles from the measured spectra. In addition to the temperature-dependent Doppler broadening, air pressure also affects the observed transition and therefore the measured shape of the line profile contains information on the abundance of the emitting constituent as a function of pressure. Thus one can estimate the vertical profile and by integrating it one can calculate the column density. Comparisons between these two column density estimation methods indicate that if ν_o in equation (1) is chosen to be 612 kHz, which means that we integrate over the range of frequencies where the line stands out clearly above the background, the two methods agree well with each other if the lower pressure level for the column is set to 0.2 hPa (~60 km). Since the air pressure increases rapidly with decreasing altitude the contribution to the observed line shape from CO emission below 60 km is sufficiently pressure broadened as to not influence the sharper line profile from the mesospheric emission. Vertical profiles and column densities have been calculated since September 2001 from the daily averaged spectra using a package based on the optimal estimation method [*Eriksson*, 2000]. Number densities of CO are retrieved with a vertical resolution of 20 km, which means that each data point is a weighted mean of the number densities in an altitude range of ~20 km centred at the altitude of the point.

4. Description of the Numerical Model

[6] The Whole Atmosphere Community Climate Model (WACCM) is a General Circulation Model developed at the National Center for Atmospheric Research (NCAR) using components from three well-validated atmospheric models. The dynamics core model is based upon the NCAR Community Atmospheric Model (CAM) [*Boville*, 1995]; it calculates explicitly the circulation and thermodynamics of the global atmosphere from the ground to about 140 km. Chemistry and related processes are simulated using the Model for OZone And Related chemical Tracers, MOZART [*Brasseur et al.*, 1998]. Additional chemical and physical processes needed to represent the mesosphere and thermosphere are taken from the Thermosphere, Ionosphere and Mesosphere Electrodynamics General Circulation Model (TIME-GCM) [*Roble and Ridley*, 1994]. A major advantage of the model for studies of the middle atmosphere is that the upper boundary is located in the lower thermosphere; this reduces the possibility of spurious reflection of planetary waves, and allows transport and chemical processes to be represented explicitly throughout the middle atmosphere. WACCM dynamical parameterisations are described by *Sassi et al.* [2002]. They include the effects of breaking gravity waves on the momentum and thermal budgets, as well as the effects of molecular diffusion. Calculation of chemical species distributions with MOZART take full account of diffusive separation of CO. The effect of vertical mixing of constituents due to gravity wave breaking can also be included. We show that this effect is relatively small unless the Prandtl number for gravity wave diffusion is close to unity. The simulations presented in this paper use "offline" chemistry; that is, dynamical fields computed with WACCM are used to transport chemical species in the MOZART chemical code, but changes in the latter do not feed back upon the dynamics through the thermo-

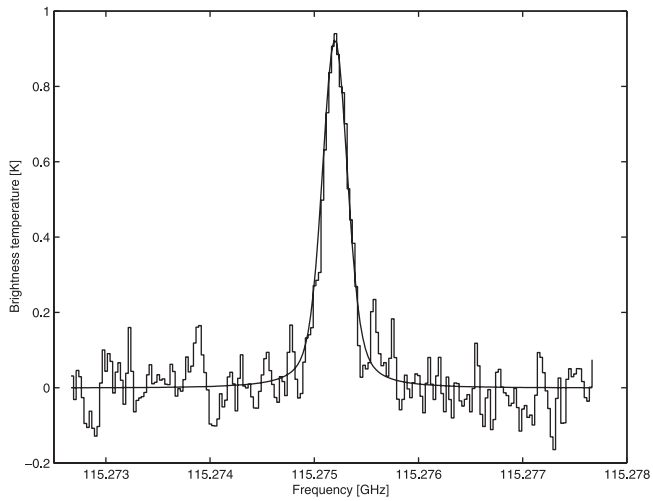

Figure 2. A spectrum corrected for the tropospheric attenuation together with a forward model fit. The channel spacing is 25 kHz. Frequency shifting is performed but in the figure only the part with the positive peak is shown.

dynamic budget. All the calculations are performed at 2.8° × 2.8° horizontal resolution, and vertical resolution that varies from ~1.25 km near the tropopause to ~3.0–3.5 km in the lower thermosphere.

5. Results and Discussion

[7] Figure 3 shows CO column estimates above 0.20 hPa (~60 km) for 1998–99, 2000–01 and 2001–02, together with WACCM results at 1-day intervals for a single year at the gridpoint (58.57°N, 11.25°E) closest to the location of Onsala. Data from *Aellig et al.* [1995] (47°N, 7.5°E) is also included for comparison. The errors in the observed CO columns are <10%. Column densities highlight CO changes below 80 km since ~80% of the estimated column is found below that altitude. The model captures the seasonal cycle of CO column abundance as well as the large intraseasonal variability. Calculated CO column amounts for the model year shown are within the interannual variability seen in the observations. In the summertime there is much less variability in the observations and rather close agreement with the model.

[8] The calculations shown in Figure 3 were made using Prandtl number Pr = 4 for the diffusivity due to breaking gravity waves. Comparison with calculations without gravity wave diffusion indicate that diffusion reduces CO column by a few percent because it acts to transport CO from its source region in the lower thermosphere to near 80 km, where it can be destroyed by reaction with OH, thus "drawing down" the thermospheric CO reservoir. In the absence of diffusion, CO builds up above 90 km during summer and is transported downward by the mean meridional circulation in winter, resulting in larger CO abundances during the winter season. A similar mechanism is discussed by *Garcia and Solomon* [1985] for atomic oxygen. Although reduction of the CO column by gravity wave diffusion is small in the Pr = 4 calculation shown in Figure 3, it can be as large as 20–25% when Pr is set to unity (not shown). This finding has bearing on the question of "effective net diffusivity" in parameterizations of gravity wave breaking [e.g., *McIntyre*, 1989]. In such parameterizations Pr quantifies the effect of mixing due to turbulent breakdown of gravity waves, the effective diffusivity being inversely proportional to Pr. Theoretical considerations [e.g., *Fritts and Dunkerton*, 1985; *Coy and Fritts*, 1988; *McIntyre*, 1989] and comparison of models and observations [e.g., *Garcia*, 1989; *Nedoluha et al.*, 1996] suggest a Pr substantially larger than unity. Our results are consistent with these studies, since calculated CO column is in better agreement with observations when Pr = 4 than when Pr = 1. However, our results are insensitive to even larger values for Pr since, as already noted, results for Pr = 4 are only slightly different from those obtained when gravity wave diffusion is neglected altogether (Pr = ∞).

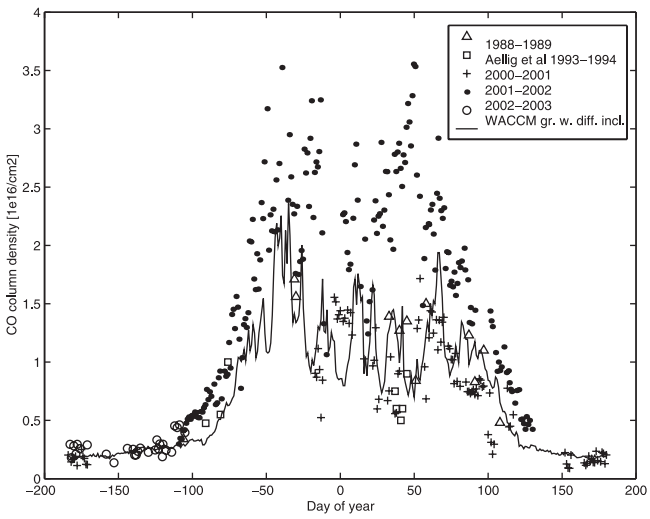

Figure 3. CO column densities [10^{16} cm^{-2}] from pressure levels lower than 0.20 hPa (above ~60 km) as a function of time. The solid curve shows WACCM results at 1-day intervals, with gravity wave diffusion included (Pr = 4).

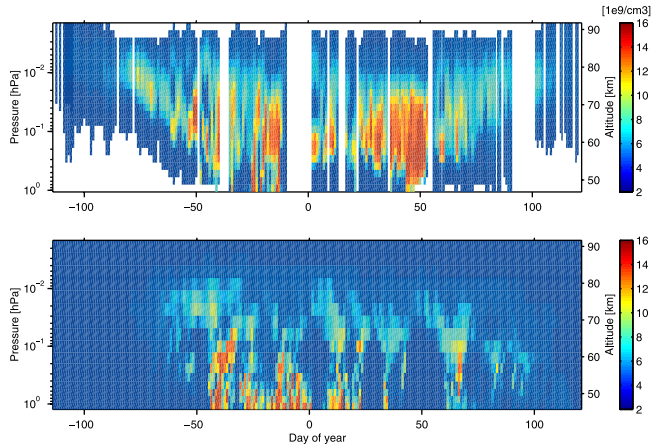

Figure 4. CO number densities [10^9 cm^{-3}] as a function of altitude and time. The upper plot shows the results from the ground based measurements from September 2001 through May 2002 and the lower plot shows the WACCM results, with gravity wave diffusion included (Pr = 4), at 1-day intervals. Measurement data are only shown for altitudes where the measurement provides most of the information, and the influence of the a priori CO profile is expected to be small.

[9] Figure 4 shows the measured variation of CO number density between September 2001 and May 2002 in the altitude range 0.8 to $2{\cdot}10^{-3}$ hPa (~50–90 km). It also shows WACCM results at 1-day intervals from the same run used to compute the column amounts in Figure 3. The expected seasonal change, with wintertime downwelling of CO-rich air from its source region in the thermosphere, is clearly seen in the observations. This behavior is well reproduced by the model, as is the large intraseasonal variability during winter.

[10] The comparisons shown in Figures 3–4 indicate that the seasonal cycle of CO calculated with WACCM is consistent with that observed at Onsala. An important feature of the data is the large intraseasonal and interannual variability in winter, which for present purposes we define as November through March. CO column amounts for 2001–2002 are about twice as large as those for 2000–2001, and in each of these winters the column varies by a factor of 2–3. WACCM simulations exhibit similar intraseasonal variability, as shown in Figure 5, which displays the results of a 21-year simulation. The ensemble mean

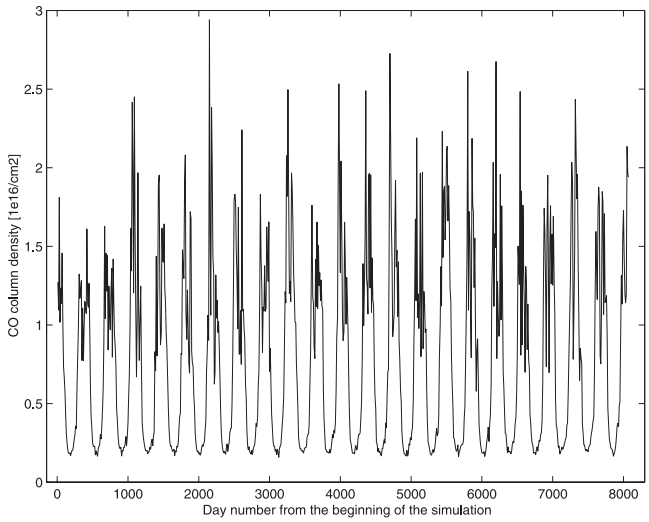

Figure 5. Calculated CO column values (in units of 10^{16} cm^{-2}) from a 21-year integration of WACCM, at a gridpoint close to the location of the Onsala site, as a function of time.

standard deviation (sd) of winter CO column for this run is $0.43 \cdot 10^{16}$ cm^{-2}, similar to the sd of the observations for 2000–01 ($0.3 \cdot 10^{16}$ cm^{-2}) and 2001–02 ($0.5 \cdot 10^{16}$ cm^{-2}). On the other hand, interannual variability is larger in the data than in the model. The ensemble mean winter CO column for the 21-year run is $1.3 \cdot 10^{16}$ cm^{-2}, and the sd of this mean is $0.12 \cdot 10^{16}$ cm^{-2}. Observed winter mean CO columns are $1.2 \cdot 10^{16}$ for 2000–01 and $3.2 \cdot 10^{16}$ cm^{-2} for 2001–02. The first of these values lies within one sd of the model's ensemble mean, but the second is ~8 sd above it. Taken at face value, this result implies that WACCM does not simulate the full range of interannual variability present in nature. However, this conclusion is tentative because the winter of 2001–02 appears to be anomalous; the very large CO column amounts observed in 2001–02 are not found in the other two seasons shown in Figure 3.

[11] Intraseasonal and interannual variability in WACCM occurs mainly in winter because it arises from meridional transport of CO-rich polar air by planetary waves, whose amplitude is highly variable within and across winters. We have ascertained that, when planetary waves displace the polar vortex over Onsala, local CO column amounts increase markedly; the reverse is true when the vortex is displaced away from Onsala. In the 21-year run, the ensemble means minimum and maximum columns in winter (which correspond to average "out-of-vortex" and "in-vortex" conditions for Onsala) are $0.73 \cdot 10^{16}$ and $2.2 \cdot 10^{16}$ cm^{-2}, respectively. The generally good agreement between observations and model calculations implies that known dynamical processes (seasonal variation of the mean meridional circulation; transport by planetary waves; gravity wave diffusion) can account for much of the magnitude and the intraseasonal variability of CO in the mesosphere. Interannual variability is larger in the data than in the model, but this finding rests on the observations for a single season (2001–02) and thus requires additional observations and further scrutiny of the data before it can be confirmed.

[12] **Acknowledgments.** We thank Richard Bevilacqua (Naval Research Laboratory, Washington) for his inspiration on this kind of measurement and Joel Elldér for his pioneering technical work. Sergey Rozanov (Lebedev Physical Institute, Moscow) improved the receiver considerably. The Swedish Natural Science Research Council financed the receiver and the European Commission supported this project.

References

Aellig, C. P., N. Kämpfer, and A. Hauchecorne, Variability of mesospheric CO in the fall and winter as observed with ground-based microwave radiometry at 115 GHz, *J. Geophys. Res.*, *100*, 14,125–14,130, 1995.

Allen, D. R., J. L. Stanford, M. A. López-Valverde, N. Nakamura, D. J. Lary, A. R. Douglass, M. C. Cerniglia, F. W. Taylor, and R. J. Wells, Observations of middle atmosphere CO from the UARS ISAMS during the early northern winter 1991/1992, *J. Atmos. Sci.*, *56*, 563–583, 1999.

Bevilacqua, R. M., A. A. Stark, and P. R. Schwartz, The variability of carbon monoxide in the terrestrial mesosphere as determined from ground based observations of the CO J = 1 → 0 emission line, *J. Geophys. Res.*, *90*, 5777–5782, 1985.

Boville, B. A., Middle atmosphere version of CCM2(MACCM2): Annual cycle and interannual variability, *J. Geophys. Res.*, *100*, 9017–9039, 1995.

Brasseur, G. P., D. A. Hauglustaine, S. Walters, P. J. Rasch, J.-F. Müller, C. Granier, and X. X. Tie, MOZART, A global chemical transport model for ozone and related chemical tracers: 1, Model description, *J. Geophys. Res.*, *103*, 28,265–28,289, 1998.

Clancy, R. T., D. O. Muhleman, and M. Allen, Seasonal variability of CO in the terrestrial mesosphere, *J. Geophys. Res.*, *89*, 9673–9676, 1984.

Coy, L., and D. C. Fritts, Gravity wave heat fluxes: A Lagrangian approach, *J. Atmos. Sci.*, *41*, 1893–1898, 1988.

Eriksson, P., Analysis and comparison of two linear regularization methods for passive atmospheric observations, *J. Geophys. Res.*, *105*, 18,157–18,167, 2000.

Forkman, P., The radio-aeronomy station at Onsala Space Observatory, *Tech. Rep. 336L*, Dep. of Radio and Space Sci. and Onsala Space Obs., Chalmers Univ. of Technol., Göteborg, Sweden, 2000.

Fritts, D. C., and T. J. Dunkerton, Fluxes of heat and constituents due to convectively unstable gravity waves, *J. Atmos. Sci.*, *42*, 549–556, 1985.

Garcia, R. R., Dynamics, radiation, and photochemistry in the mesosphere: Implications for the formation of noctilucent clouds, *J. Geophys. Res.*, *94*, 14,605–14,615, 1989.

Garcia, R. R., and S. Solomon, The effect of breaking gravity waves on the dynamics and chemical composition of the mesosphere and lower thermosphere, *J. Geophys. Res.*, *90*, 3850–3868, 1985.

Garcia, R. R., F. Stordal, S. Solomon, and J. T. Kiehl, A new numerical model of the middle atmosphere: 1. Dynamics and transport of tropospheric source gases, *J. Geophys. Res.*, *97*, 12,967–12,991, 1992.

López-Puertas, M., M. A. López-Valverde, R. R. Garcia, and R. G. Roble, A review of CO_2 and CO abundances in the middle atmosphere, in *Atmospheric Science Across the Stratopause*, *Geophys. Monogr. Ser.*, vol. 123, edited by D. E. Siskind, S. D. Eckermann, and M. E. Summers, pp. 83–100, AGU, Washington, D. C., 2000.

McIntyre, M. E., On dynamics and transport near the polar mesopause in summer, *J. Geophys. Res.*, *94*, 14,617–14,628, 1989.

Nedoluha, G. E., R. M. Bevilacqua, R. M. Gomez, W. B. Waltman, B. C. Hicks, D. L. Thacker, and W. A. Matthews, Measurements of water vapor in the middle atmosphere and implications for mesospheric transport, *J. Geophys. Res.*, *101*, 21,183–21,194, 1996.

Roble, R. G., and E. C. Ridley, A thermosphere-ionosphere-mesosphere-electrodynamics general circulation model (TIME-GCM): Equinox solar cycle minimum simulations (30–500 km), *Geophys. Res. Lett.*, *21*, 417–420, 1994.

Sassi, F., R. R. Garcia, B. A. Boville, and H. Liu, On temperature inversions and the mesospheric surf zone, *J. Geophys. Res.*, *107*(D19), 4380, doi:10.1029/2001JD001525, 2002.

P. Eriksson, P. Forkman, and A. Winnberg, Onsala Space Observatory, Centre for Astrophysics and Space Science, Chalmers University of Technology, SE-439 92 Onsala, Sweden. (forkman@oso.chalmers.se)

R. R. Garcia and D. Kinnison, Atmospheric Chemistry Division, National Center for Atmospheric Research, 1850 Table Mesa Drive, Boulder, CO 80305, USA.